COBEM 2023 27TH INTERNATIONAL CONGRESS OF MECHANICAL ENGENEERING

ABCM Brazilian Society of Mechanical Sciences and Engineering
27th ABCM International Congress of Mechanical Engineering
December 04-08, 2023, Florianópolis-SC, Brazil

COB-2023-0538
CHARACTERIZATION OF INTERMITTENT EXTREME EVENTS IN ADIABATIC AND ISOTHERMAL SUPERSONIC TURBINE CASCADES

Gabriel Y. R. Hamada
William R. Wolf
University of Campinas, Campinas, SP, 13083-860, Brazil
g265310@unicamp.br
wolf@fem.unicamp.br

Hugo F. S. Lui
University of Campinas, Campinas, SP, 13083-860, Brazil
hugo.slui@gmail.com

Tulio R. Ricciardi
University of Illinois Urbana-Champaign, Urbana, IL, 61801, USA
tricci@illinois.edu

Carlos Junqueira-Junior
Arts et Métiers Institute of Technology, DynFluid, CNAM, HESAM University, 151 Boulevard de l'Hôpital, 75013, Paris, France
junior.junqueira@ensam.eu

Abstract. *We investigate extreme events occurring in the shock-boundary layer interactions (SBLIs) of a supersonic turbine cascade. The present analysis is performed considering adiabatic and isothermal blades, where for the latter the wall to inlet temperature ratio is* $T_w/T_\infty = 0.75$*, representing a cooled wall. The supersonic flows are computed by wall-resolved large eddy simulations (LES) for an inlet Mach number* $M_\infty = 2.0$ *and Reynolds number based on the axial chord* $Re = 2 \times 10^5$*. Different incident shock wave topologies are observed on the suction and pressure sides of the airfoil. For the former, an oblique shock impinges on the boundary layer leading to a more pronounced separation bubble. On the other hand, for the latter, a normal shock forms in a Mach reflection, inducing a small separation bubble near the wall. Results are presented in terms of the conditional proper orthogonal decomposition (CPOD) modes for the tangential and normal velocity components, as well as pressure. These modes are presented for three different time instants to characterize the cause and effect of the extreme events in the flowfield.*

Keywords: *Shock boundary layer interaction, LES, supersonic turbine, CPOD*

1. INTRODUCTION

Supersonic turbines find application in high-speed propulsion and power generation systems (Paniagua *et al.*, 2014; Sousa *et al.*, 2017) and the interactions between shocks and boundary layers pose a challenge for the design of these fluid machinery. Typically, the shock-boundary layer interactions (SBLIs) arise due to the shock waves that form at the stator/rotor leading edges, and which subsequently impinge on the boundary layers of the neighboring airfoils. The shocks impose intense adverse pressure gradients on the boundary layers that cause flow separation and may lead to the formation of separation and reattachment shocks. The entire shock system induces strong pressure fluctuations and intense thermal loading which can compromise the turbine structural integrity and reduce the overall efficiency of the machinery (Delery, 1985; Babinsky and Harvey, 2011; Gaitonde, 2015; Klinner *et al.*, 2019; Spottswood *et al.*, 2019; Sandberg and Michelassi, 2022).

The typical spectrum of SBLIs is broadband, composed of low and mid-frequency tonal peaks. On one hand, the separated flow and its shock system induce the low-frequency dynamics which are related to the oscillations of the separation bubble and the motions of separation and reattachment shocks. On the other hand, a broad range of frequencies is excited by the incoming turbulent boundary layer (Clemens and Narayanaswamy, 2014; Dussauge *et al.*, 2006). Several authors have studied the low-frequency events taking place in SBLIs using experimental (Dussauge *et al.*, 2006; Dupont *et al.*, 2006; Ganapathisubramani *et al.*, 2009; Piponniau *et al.*, 2009; Combs *et al.*, 2018; Murphree *et al.*, 2021) and numerical (Pirozzoli and Grasso, 2006; Wu and Martín, 2008; Touber and Sandham, 2009; Priebe and Martín, 2012; Morgan *et al.*, 2013; Aubard *et al.*, 2013; Bermejo-Moreno *et al.*, 2014; Agostini *et al.*, 2015; Adler and Gaitonde, 2018; Vyas *et al.*, 2019; Adler and Gaitonde, 2020; Hu *et al.*, 2021; Deshpande and Poggie, 2021; Bugeat *et al.*, 2022) techniques. In these

studies, the sources of low-frequency dynamics have been the subject of debate because their driving mechanisms have not been fully characterized (Clemens and Narayanaswamy, 2014).

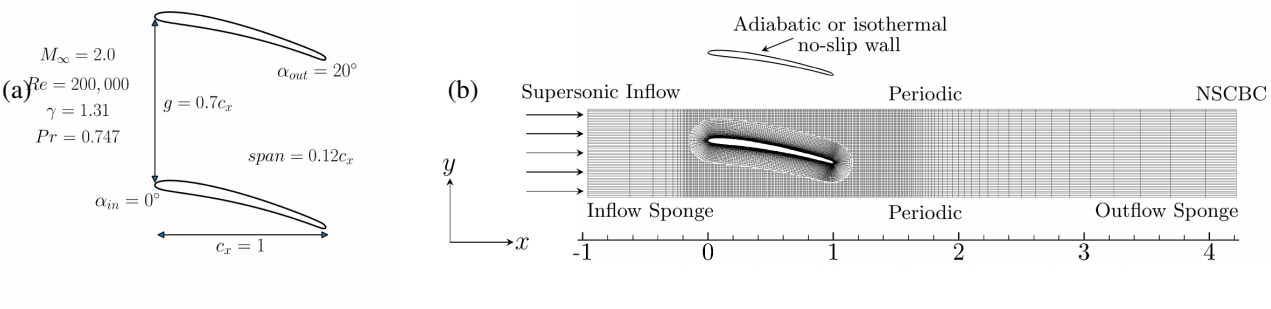

Figure 1: Schematics of (a) flow configuration and geometrical parameters, and (b) computational domain skipping every 5 grid points.

Recently, Lui *et al.* (2022b) performed wall-resolved large-eddy simulations (LES) to investigate the dynamics of SBLIs taking place in a supersonic turbine cascade. These authors showed that large-scale streaky structures disturbed the separation bubble which, in turn, would cause the motion of the reflected shock. In the simulations, coherent structures in the boundary layer were amplified at the frequency of the bubble breathing and shock motion. In the same work, proper orthogonal decomposition (POD) was employed to identify the spatial structures that oscillated at low frequencies. Lui *et al.* (2022a) and Hamada *et al.* (2023) investigated how the blade thermal boundary conditions affected the low-frequency dynamics and the turbulence statistics. It was shown that the bubble size and the turbulence statistics depicted different behavior for adiabatic and isothermal walls. Lastly, Lui *et al.* (2023) performed LES for different inlet Mach numbers to assess this parameter influence in the bubble dynamics. These authors observed that, as the Mach number increases, the suction side low-frequency regions with high-amplitude spectral energy moved downstream in the axial direction, and the SBLI systems excited even lower frequencies when scaled by the axial chord and inlet velocity.

In this work we utilize the same LES simulations used in Hamada *et al.* (2023) and Lui *et al.* (2022a), and employ a data-driven post-processing technique well suited for the analysis of extreme intermittent events. The condition proper orthogonal decomposition (CPOD) (Schmidt and Schmid, 2019; Stahl *et al.*, 2022) is employed to investigate cause and effect of intermittent events that occur in the SBLIs taking place in supersonic turbine cascades with adiabatic and isothermal (cooled) blades.

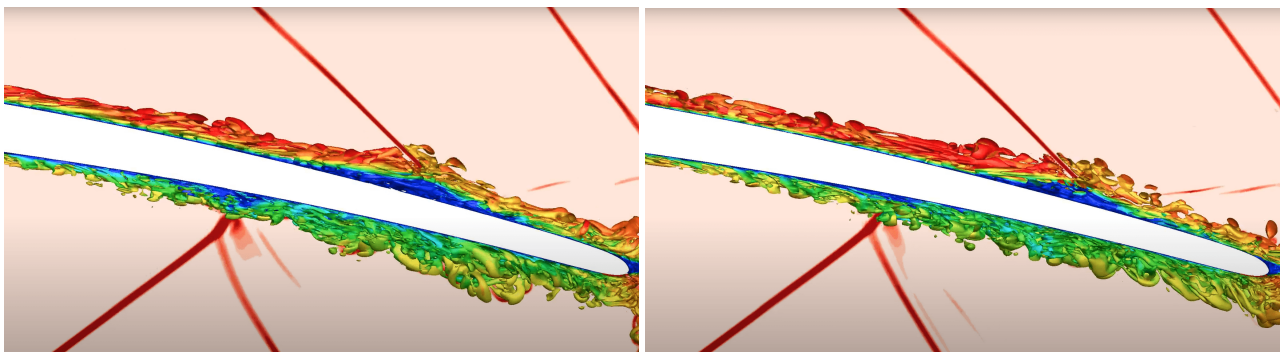

(a) Adiabatic (b) Cooled

Figure 2: Iso-surfaces of Q-criterion colored by u-velocity component for different boundary conditions. The background plane displays the shock waves by visualizing the density gradient magnitude $|\nabla\rho|$.

2. THEORETICAL FORMULATION AND NUMERICAL METHODOLOGY

Large eddy simulations with wall resolution are employed to solve the compressible Navier-Stokes equations in a curvilinear system written in terms of the contravariant velocity components. Assuming the gas to be calorically perfect, the set of equations is closed by the equation of state. The equations are solved in nondimensional form where the length, velocity components, density, pressure, temperature and time are nondimensionalized by the axial airfoil chord c_x, inlet speed of sound a_∞, inlet density ρ_∞, $\rho_\infty a_\infty^2$, $(\gamma-1)\,T_\infty$ and c_x/a_∞, respectively. The Reynolds and Mach numbers are calculated as $Re = \rho_\infty U_\infty c_x/\mu_\infty$ and $M_\infty = U_\infty/a_\infty$, respectively, where the U_∞, T_∞ and μ_∞ represent the flow velocity, temperature and dynamic viscosity coefficient computed at the cascade inlet. The Prandtl number is given by $Pr = \mu_\infty c_p/\kappa_\infty$, where c_p is the specific heat at constant pressure and κ_∞ is the inlet thermal conductivity. The viscosity

is computed using the nondimensional Sutherland's law.

The spatial discretization of the governing equations is performed using a sixth-order accurate compact scheme (Nagarajan *et al.*, 2003) implemented on a staggered grid. A sixth-order compact interpolation method is also used to obtain fluid properties on the staggered nodes. A sixth-order compact filter Lele (1992) is applied in flow regions far away from solid boundaries at each time step to control numerical instabilities which may arise from mesh distortion and stretching, and interpolations between overlapping grids. As discussed by Mathew *et al.* (2003), an explicit subgrid scale model is not applied.

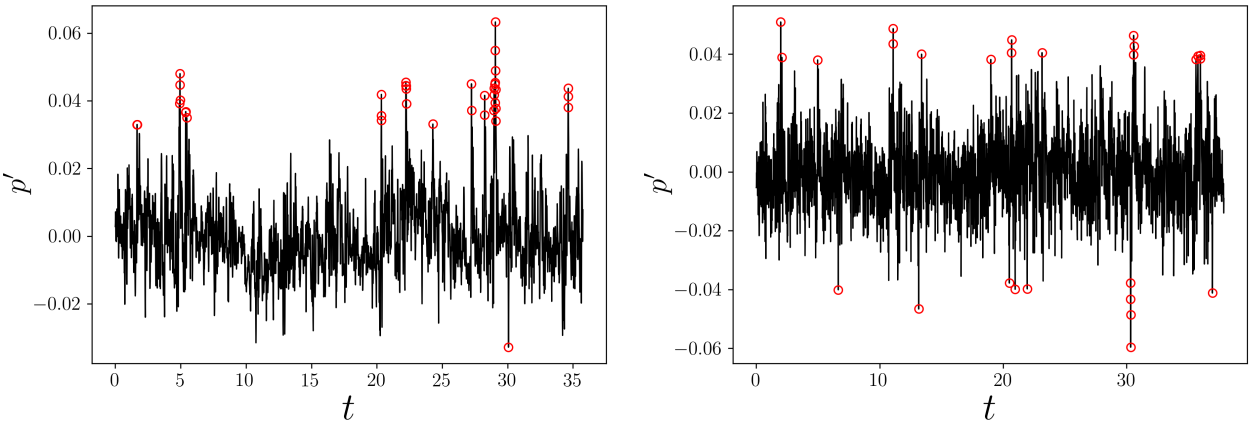

(a) Adiabatic

(b) Cooled

Figure 3: Pressure fluctuation in the airfoil surface for the selected probes. The red circles are the extreme events observed with three standard deviation.

Two grids are employed in the present simulations: one is a body-fitted O-grid block which surrounds the blade and the other is a Cartesian block employed to facilitate the implementation of the pitchwise periodicity. In the O-grid, the time integration of the equations is carried out by the implicit second-order scheme of Beam and Warming (1978) to reduce the stiffness problem typical of boundary layer grids. In the background Cartesian block, a third-order Runge-Kutta scheme is used for time advancement of the Navier-Stokes equations. A fourth-order Hermite interpolation scheme (Bhaskaran and Lele, 2010) is used to exchange information between grid blocks in the overlapping zones. Further details about the numerical procedure can be found in Refs. (Nagarajan *et al.*, 2003; Bhaskaran, 2010; Wolf, 2011). The code has been previously validated for simulations of unsteady compressible flows Bhaskaran (2010); Wolf *et al.* (2012); Lui *et al.* (2022b), including the flow through a turbine cascade Bhaskaran and Lele (2010).

The localized artificial diffusivity (LAD) (Cook, 2007) is used to compute an artificial dissipation along shock waves. The specific implementation employed is the method LAD-D2-0 proposed by Kawai *et al.* (2010) with no artificial shear viscosity. To promote the transition to turbulence on the airfoil boundary layers, an artificial body force is included in the momentum and energy equations, where a time-periodic unsteady actuation and random spanwise treatment are assumed. The forcing is applied along the wall-normal region up to a distance of $0.001c_x$ at $0.22 < x < 0.27$ on the suction side, and at $0.10 < x < 0.15$ on the pressure side, with the actuation changing every $\Delta t \approx 0.003$ in a spanwise-random fashion.

For the CPOD, the detailed formulation can be found in the work from Schmidt and Schmid (2019) and Stahl *et al.* (2022). Here, the CPOD technique is applied as a post-processing tool of the LES dataset. This variation of the POD is selected due to its capability of isolating cause and consequence for selected intermittent events.

3. FLOW AND MESH CONFIGURATIONS

This section presents details of the flow configurations investigated and the computational grids employed in the LES calculations. Figure 1 (a) shows the flow conditions and geometrical parameters. The inlet Mach number is M_∞ = 2.0 and the Reynolds number based on the inlet velocity and airfoil axial chord is $Re = 2 \times 10^5$. Further information can be obtained in the references of Lui *et al.* (2022a) and Hamada *et al.* (2023).

Figure 1 (b) displays a schematic of the overset grid employed in the LES along with the implemented boundary conditions. The O-grid block has $1200 \times 280 \times 144$ points and it is embedded in the background Cartesian grid block of size $960 \times 280 \times 72$. Therefore, the grid has approximately 68 million points. Depending on the case, adiabatic or isothermal boundary conditions are applied along the blade surface. For the latter, the wall to inlet temperature ratio is $T_w/T_\infty = 0.75$, representing a cooled wall. The boundary conditions are the supersonic inflow for the inlet and the

Navier-Stokes characteristic boundary condition (NSCBC) (Poinsot and Lele, 1992) for the outlet. A damping sponge is also applied near the inflow and outflow boundaries to minimize reflections of numerical disturbances (Israeli and Orszag, 1981; Nagarajan *et al.*, 2003). Periodic boundary conditions are used in the y-direction of the background grid and in the spanwise direction, in order to simulate a linear cascade of blades and to enforce a statistically homogeneous flow along the span, respectively. The simulation is initialized with a uniform flow and statistics are computed after the initial transients are discarded.

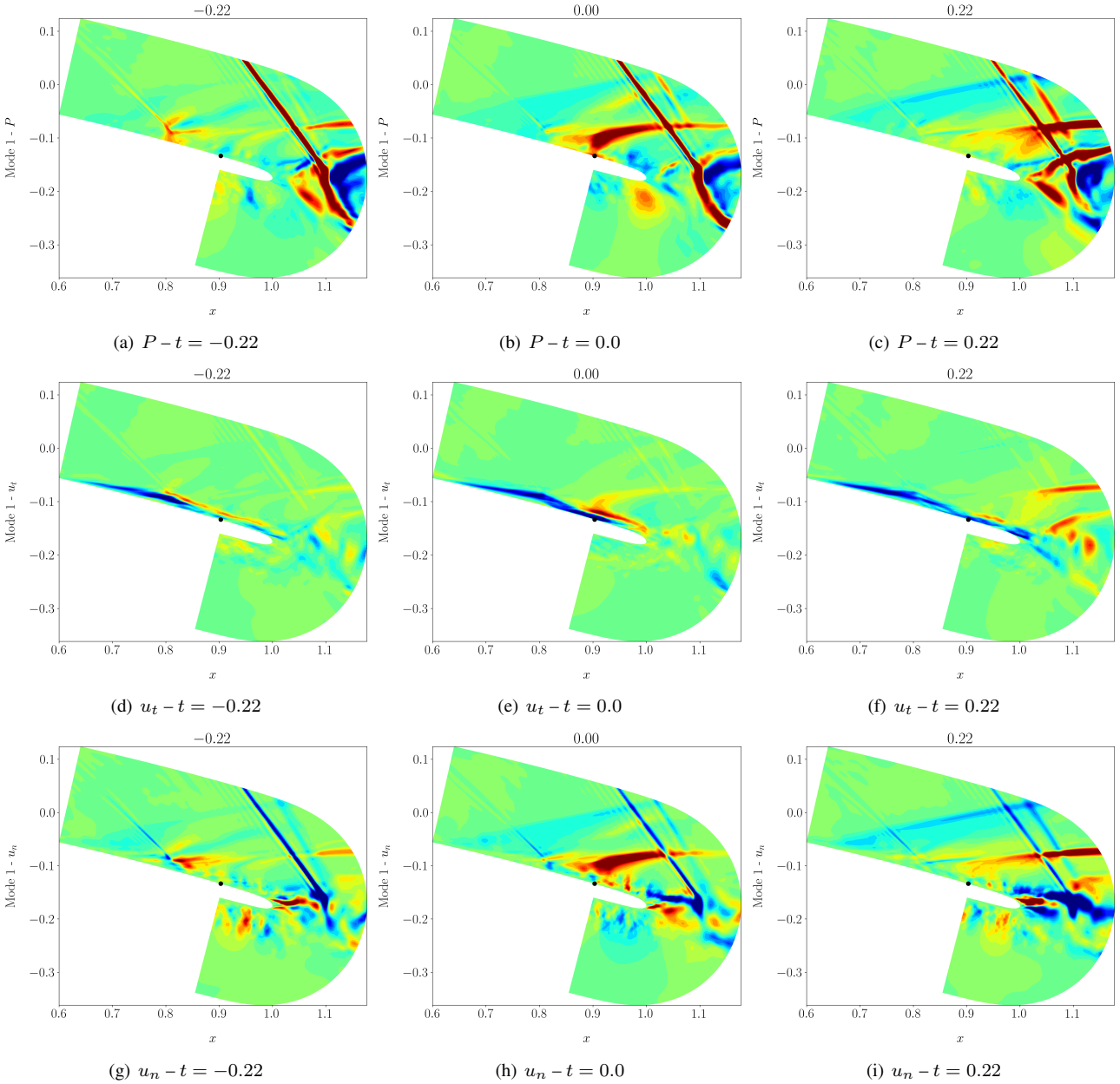

(a) $P-t=-0.22$ (b) $P-t=0.0$ (c) $P-t=0.22$

(d) $u_t-t=-0.22$ (e) $u_t-t=0.0$ (f) $u_t-t=0.22$

(g) $u_n-t=-0.22$ (h) $u_n-t=0.0$ (i) $u_n-t=0.22$

Figure 4: CPOD modes before, during, and after the event for the adiabatic case. The first CPOD mode for the pressure, tangential and normal velocity components are shown. The black dot represents the probe location, whose signal is plotted in Fig. 3 (a). The colors levels are evenly distributed from -0.001 to 0.001, and they show the fluctuations from the mean for the plotted properties.

4. RESULTS

Flow snapshots are shown in Fig. 2 with the iso-surfaces of Q-criterion colored by u-velocity to represent the turbulent structures around the SBLI. The magnitude of the density gradient is also shown in red to highlight the shock-waves. The impinging shocks observed on both sides of the blade come from detached oblique shock waves that form in front of the leading edge of the neighboring blades. On the suction side, an oblique shock impinges on the turbulent boundary layer, which causes flow detachment leading to a recirculation zone. A similar phenomenon is observed on the pressure side, but

the incident shock becomes a Mach reflection that forms a normal shock near the wall. Figs. 2 (a) and (b) show detailed views of the separation bubbles for the adiabatic and cooled wall cases, respectively. It can be observed that cooling the wall results in a smaller recirculation zone, depicted by the deep blue color regions on the suction and pressure sides of the turbine.

The extreme events are selected through observation of pressure fluctuations in the airfoil surface (Fig. 3). We consider that an event is extreme when its peak exceeded three standard deviations from the mean value and, in this work, only the positive extremes are considered.

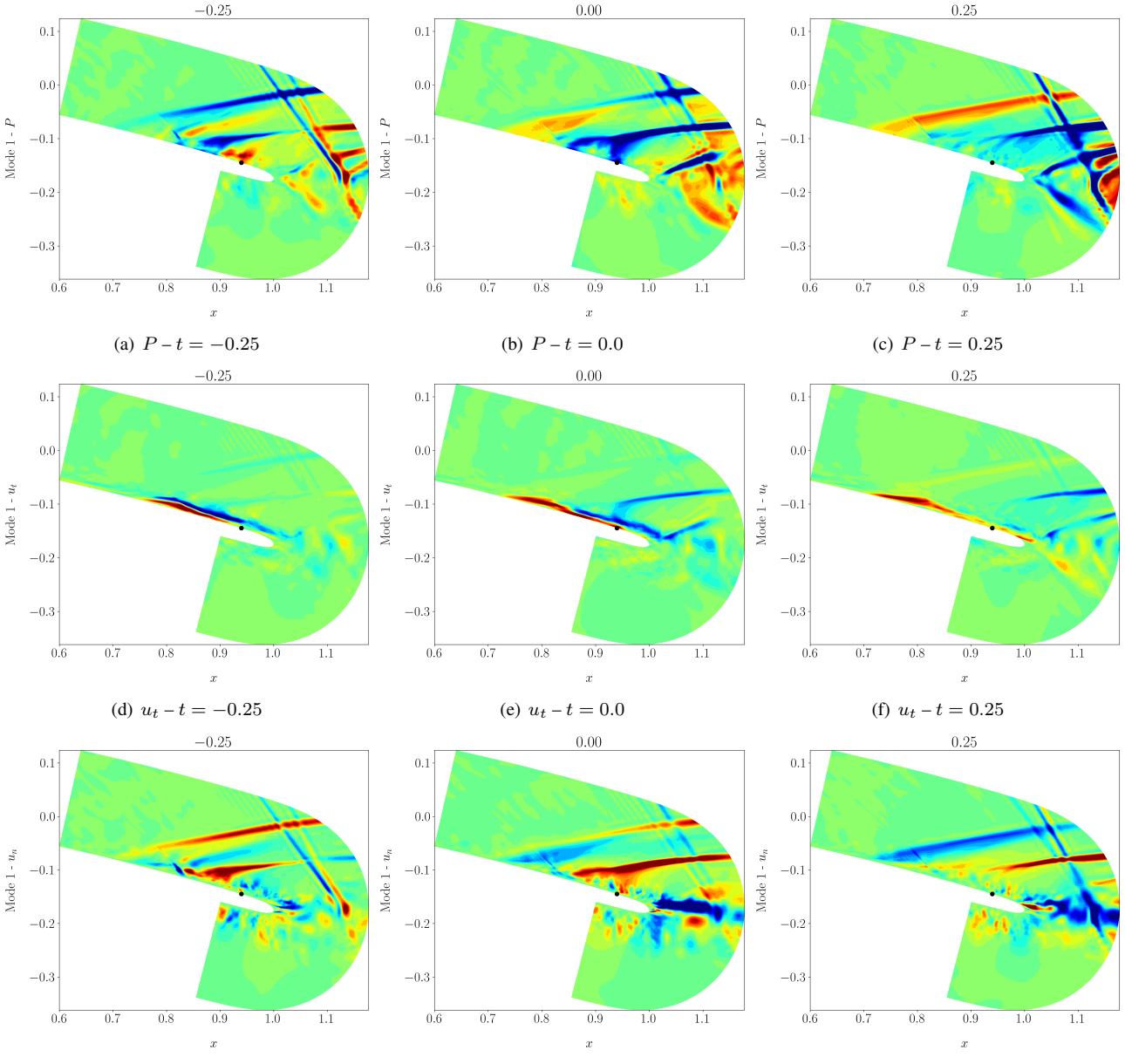

(a) $P - t = -0.25$ (b) $P - t = 0.0$ (c) $P - t = 0.25$

(d) $u_t - t = -0.25$ (e) $u_t - t = 0.0$ (f) $u_t - t = 0.25$

(g) $u_n - t = -0.25$ (h) $u_n - t = 0.0$ (i) $u_n - t = 0.25$

Figure 5: CPOD modes before, during, and after the event for the cooled case. The first CPOD mode for the pressure, tangential and normal velocity are shown. The black dot represent the probe location, whose signal is plotted in Fig. 3 (b). The colors levels are evenly distributed from -0.001 to 0.001, and they show the fluctuations from the mean for the plotted properties.

Three time instants (one just before, one at the specific event instant, and one just after its occurrence) are plotted for pressure, and tangential and normal velocity components in Fig. 4. The colors levels are evenly distributed from -0.001 to 0.001, and they show the fluctuations from the mean for the plotted properties. Looking at Figs. 4 (b), (e) and (h), it can be seen that in the instant of the event, there is a large disturbance, which resembles a reflection shock in the pressure probe, passing over the probe (black dot). In Fig. 4 (e), the tangential velocity mode shows a strong shearing structure over the probe.

The large velocity and pressure disturbances that are advected over the probe at $t = 0.0$ can be tracked to provide a further analysis of the mechanisms that originate in the shock-bubble region in Figs. 4 (a), (d) and (g), near $x = 0.8$. The disturbances arise from the boundary layer upstream of the SBLI zone and perturb the impinging shock, propagating through the shear layer and in the reattachment shock. The consequence of this large structure can be seen in Figs. 4 (c), (f) and (i). The flow perturbation upstream the probe, at the SBLI region, is transported downstream and reaches the trailing edge, heavily affecting this region by expelling structures in different directions (two bright red elongated structures observed near the trailing edge for the pressure mode between $1.0 < x < 1.1$). These structures can reach and affect the reflection shock that comes from the pressure side of the neighboring blade.

The CPOD modes for the cooled case are plotted in Fig. 5. Differently from the adiabatic case, in the cooled wall the shock structures are more enhanced. In general, it seems that the same mechanism observed in the adiabatic case is responsible for the extreme events in the cooled case, and this deserves further investigations.

Now, looking exclusively to the CPOD modes of tangential velocity for both cases, the shear layer after the bubble is constantly present, and when the larger pressure fluctuation occurs, the shear layer influence reaches further downstream leading to the extreme event. Further analysis is necessary but there is a possibility that these extreme events are related to the low-frequency bubble motion observed in Lui *et al.* (2022b,a). Differently from the snapshots obtained from the simulation, in the CPOD modes it is possible to observe the separation and reflection shocks and how they are influenced from the extreme events.

5. CONCLUSIONS

Large eddy simulations are performed to investigate the effects of thermal boundary conditions on SBLIs and their low-frequency intermittent events for a supersonic turbine cascade. The simulations are performed for an inlet Mach number of $M_\infty = 2.0$ and Reynolds number $Re = 200000$. Adiabatic and isothermal boundary conditions are analyzed, where for the latter, the wall to inlet temperature ratio is $T_w/T_\infty = 0.75$.

Snapshots are shown in terms of iso-surfaces of Q-criterion colored by u-velocity to visualize the separation regions, and the density gradient magnitude displays the shock waves. Extreme events are selected using three standard deviations from the mean for the wall-pressure fluctuation on the blade suction side after the separation bubble and only positive events are utilized. The CPOD modes are plotted for three different instants of the event, before, during and after the extreme event. The colors represent the fluctuations from the mean for the selected variables. It was shown that the extreme events can be attributed to a structure advected upstream of the SBLI zone, which hits the impinging shock and propagates through the shear layer and the reattachment shock. The effects of the event can be observed in the trailing edge flow and its influence reaches the reflection shock from the pressure side of the neighboring blades, way downstream of the trailing edge.

Similar events can be observed for both thermal boundary conditions, leading to the conclusion that the extreme events are independent of the cooling effects on the blade. Lastly, the extreme event propagates downstream in the shear layer and its origin may be associated to the low-frequency dynamics of the separation bubble.

6. ACKNOWLEDGEMENTS

The authors acknowledge Fundação de Amparo à Pesquisa do Estado de São Paulo, FAPESP, for supporting the present work under research grants No. 2013/08293-7, 2019/26196-5, 2021/06448-0 and 2022/00464-6. This work was granted access to the HPC resources of IDRIS, TGCC, and CINES under the allocation A0132A12067 made by GENCI.

7. REFERENCES

Adler, M.C. and Gaitonde, D.V., 2018. "Dynamic linear response of a shock/turbulent-boundary-layer interaction using constrained perturbations". *Journal of Fluid Mechanics*, Vol. 840, p. 291–341. doi:10.1017/jfm.2018.70.

Adler, M.C. and Gaitonde, D.V., 2020. "Dynamics of strong swept-shock/turbulent-boundary-layer interactions". *Journal of Fluid Mechanics*, Vol. 896, p. A29. doi:10.1017/jfm.2020.334.

Agostini, L., Larchevêque, L. and Dupont, P., 2015. "Mechanism of shock unsteadiness in separated shock/boundary-layer interactions". *Physics of Fluids*, Vol. 27, No. 12, p. 126103. doi:10.1063/1.4937350.

Aubard, G., Gloerfelt, X. and Robinet, J.C., 2013. "Large-eddy simulation of broadband unsteadiness in a shock/boundary-layer interaction". *AIAA Journal*, Vol. 51, No. 10, pp. 2395–2409. doi:10.2514/1.J052249.

Babinsky, H. and Harvey, J., 2011. *Shock Wave-Boundary-Layer Interactions*. Cambridge Aerospace Series. Cambridge University Press, Cambridge, UK. doi:10.1017/CBO9780511842757.

Beam, R.M. and Warming, R.F., 1978. "An implicit factored scheme for the compressible Navier-Stokes equations". *AIAA Journal*, Vol. 16, No. 4, pp. 393–402. ISSN 0001-1452.

Bermejo-Moreno, I., Campo, L., Larsson, J., Bodart, J., Helmer, D. and Eaton, J., 2014. "Confinement effects in shock wave/turbulent boundary layer interactions through wall-modelled large-eddy simulations". *Journal of Fluid Mechan-*

ics, Vol. 758, p. 5–62. doi:10.1017/jfm.2014.505.

Bhaskaran, R. and Lele, S.K., 2010. "Large eddy simulation of free-stream turbulence effects on heat transfer to a high-pressure turbine cascade". *Journal of Turbulence*, Vol. 11, p. N6.

Bhaskaran, R., 2010. *Large eddy simulation of high pressure turbine cascade*. Ph.D. thesis, Stanford University.

Bugeat, B., Robinet, J.C., Chassaing, J.C. and Sagaut, P., 2022. "Low-frequency resolvent analysis of the laminar oblique shock wave/boundary layer interaction". *Journal of Fluid Mechanics*, Vol. 942, p. A43. doi:10.1017/jfm.2022.390.

Clemens, N.T. and Narayanaswamy, V., 2014. "Low-frequency unsteadiness of shock wave/turbulent boundary layer interactions". *Annual Review of Fluid Mechanics*, Vol. 46, No. 1, pp. 469–492. doi:10.1146/annurev-fluid-010313-141346.

Combs, C.S., Lash, E.L., Kreth, P.A. and Schmisseur, J.D., 2018. "Investigating unsteady dynamics of cylinder-induced shock-wave/transitional boundary-layer interactions". *AIAA Journal*, Vol. 56, No. 4, pp. 1588–1599. doi:10.2514/1.J056553.

Cook, A.W., 2007. "Artificial fluid properties for large-eddy simulation of compressible turbulent mixing". *Physics of Fluids*, Vol. 19, No. 5, p. 055103.

Delery, J.M., 1985. "Shock wave/turbulent boundary layer interaction and its control". *Progress in Aerospace Sciences*, Vol. 22, No. 4, pp. 209–280. ISSN 0376-0421. doi:https://doi.org/10.1016/0376-0421(85)90001-6.

Deshpande, A.S. and Poggie, J., 2021. "Large-scale unsteadiness in a compression ramp flow confined by sidewalls". *Phys. Rev. Fluids*, Vol. 6, p. 024610. doi:10.1103/PhysRevFluids.6.024610.

Dupont, P., Haddad, C. and Debiève, J.F., 2006. "Space and time organization in a shock-induced separated boundary layer". *Journal of Fluid Mechanics*, Vol. 559, p. 255–277. doi:10.1017/S0022112006000267.

Dussauge, J.P., Dupont, P. and Debiève, J.F., 2006. "Unsteadiness in shock wave boundary layer interactions with separation". *Aerospace Science and Technology*, Vol. 10, No. 2, pp. 85–91. ISSN 1270-9638. doi:https://doi.org/10.1016/j.ast.2005.09.006.

Gaitonde, D.V., 2015. "Progress in shock wave/boundary layer interactions". *Progress in Aerospace Sciences*, Vol. 72, pp. 80–99. ISSN 0376-0421. doi:https://doi.org/10.1016/j.paerosci.2014.09.002.

Ganapathisubramani, B., Clemens, N.T. and Dolling, D.S., 2009. "Low-frequency dynamics of shock-induced separation in a compression ramp interaction". *Journal of Fluid Mechanics*, Vol. 636, p. 397–425. doi:10.1017/S0022112009007952.

Hamada, G.Y., Lui, H., Wolf, W., Ricciardi, T. and Junqueira-Junior, C.A., 2023. "Thermal boundary condition effects on shock boundary layer interactions of a supersonic turbine cascade". In *AIAA AVIATION 2023 Forum*. p. 3697.

Hu, W., Hickel, S. and van Oudheusden, B.W., 2021. "Low-frequency unsteadiness mechanisms in shock wave/turbulent boundary layer interactions over a backward-facing step". *Journal of Fluid Mechanics*, Vol. 915, p. A107. doi:10.1017/jfm.2021.95.

Israeli, M. and Orszag, S.A., 1981. "Approximation of radiation boundary conditions". *Journal of Computational Physics*, Vol. 41, No. 1, pp. 115 – 135. ISSN 0021-9991.

Kawai, S., Shankar, S.K. and Lele, S.K., 2010. "Assessment of localized artificial diffusivity scheme for large-eddy simulation of compressible turbulent flows". *Journal of Computational Physics*, Vol. 229, No. 5, pp. 1739–1762. ISSN 0021-9991.

Klinner, J., Hergt, A., Grund, S. and Willert, C.E., 2019. "Experimental investigation of shock-induced separation and flow control in a transonic compressor cascade". *Experiments in Fluids*, Vol. 60, p. 96.

Lele, S.K., 1992. "Compact finite difference schemes with spectral-like resolution". *Journal of Computational Physics*, Vol. 103, No. 1, pp. 16–42. ISSN 0021-9991.

Lui, H., Ricciardi, T.R., Wolf, W. and Junqueira, C.A., 2022a. "Comparison of shock-boundary layer interactions in adiabatic and isothermal supersonic turbine cascades". In *AIAA AVIATION 2022 Forum*. p. 4133.

Lui, H.F.S., Ricciardi, T.R., Wolf, W.R., Braun, J., Rahbari, I. and Paniagua, G., 2022b. "Unsteadiness of shock-boundary layer interactions in a Mach 2.0 supersonic turbine cascade". *Physical Review Fluids*, Vol. 7, No. 9, p. 094602.

Lui, H., Ricciardi, T., Wolf, W. and Gaitonde, D.V., 2023. "Effect of inlet mach number on shock-boundary layer interactions in a supersonic turbine cascade". In *AIAA AVIATION 2023 Forum*. p. 3699.

Mathew, J., Lechner, R., Foysi, H., Sesterhenn, J. and Friedrich, R., 2003. "An explicit filtering method for large eddy simulation of compressible flows". *Physics of fluids*, Vol. 15, No. 8, pp. 2279–2289.

Morgan, B., Duraisamy, K., Nguyen, N., Kawai, S. and Lele, S.K., 2013. "Flow physics and RANS modelling of oblique shock/turbulent boundary layer interaction". *Journal of Fluid Mechanics*, Vol. 729, p. 231–284. doi:10.1017/jfm.2013.301.

Murphree, Z.R., Combs, C.S., Yu, W.M., Dolling, D.S. and Clemens, N.T., 2021. "Physics of unsteady cylinder-induced shock-wave/transitional boundary-layer interactions". *Journal of Fluid Mechanics*, Vol. 918, p. A39. doi:10.1017/jfm.2021.369.

Nagarajan, S., Lele, S.K. and Ferziger, J.H., 2003. "A robust high-order compact method for large eddy simulation". *Journal of Computational Physics*, Vol. 191, No. 2, pp. 392–419. ISSN 0021-9991.

Paniagua, G., Iorio, M., Vinha, N. and Sousa, J., 2014. "Design and analysis of pioneering high supersonic axial turbines". *International Journal of Mechanical Sciences*, Vol. 89, pp. 65 – 77. ISSN 0020-7403.

Piponniau, S., Dussauge, J.P., Debiève, J.F. and Dupont, P., 2009. "A simple model for low-frequency unsteadiness in shock-induced separation". *Journal of Fluid Mechanics*, Vol. 629, p. 87–108. doi:10.1017/S0022112009006417.

Pirozzoli, S. and Grasso, F., 2006. "Direct numerical simulation of impinging shock wave/turbulent boundary layer interaction at M=2.25". *Physics of Fluids*, Vol. 18, No. 6, p. 065113. doi:10.1063/1.2216989.

Poinsot, T.J. and Lele, S.K., 1992. "Boundary conditions for direct simulations of compressible viscous flows". *Journal of Computational Physics*, Vol. 101, No. 1, pp. 104 – 129. ISSN 0021-9991.

Priebe, S. and Martín, M.P., 2012. "Low-frequency unsteadiness in shock wave–turbulent boundary layer interaction". *Journal of Fluid Mechanics*, Vol. 699, p. 1–49. doi:10.1017/jfm.2011.560.

Sandberg, R.D. and Michelassi, V., 2022. "Fluid dynamics of axial turbomachinery: Blade- and stage-level simulations and models". *Annual Review of Fluid Mechanics*, Vol. 54, No. 1, pp. 255–285. doi:10.1146/annurev-fluid-031221-105530.

Schmidt, O.T. and Schmid, P.J., 2019. "A conditional space–time pod formalism for intermittent and rare events: example of acoustic bursts in turbulent jets". *Journal of Fluid Mechanics*, Vol. 867, p. R2.

Sousa, J., Paniagua, G. and Morata, E.C., 2017. "Thermodynamic analysis of a gas turbine engine with a rotating detonation combustor". *Applied Energy*, Vol. 195, pp. 247 – 256. ISSN 0306-2619.

Spottswood, S.M., Beberniss, T.J., Eason, T.G., Perez, R.A., Donbar, J.M., Ehrhardt, D.A. and Riley, Z.B., 2019. "Exploring the response of a thin, flexible panel to shock-turbulent boundary-layer interactions". *Journal of Sound and Vibration*, Vol. 443, pp. 74–89. ISSN 0022-460X. doi:https://doi.org/10.1016/j.jsv.2018.11.035. URL `https://www.sciencedirect.com/science/article/pii/S0022460X18307971`.

Stahl, S., Prasad, C., Goparaju, H. and Gaitonde, D., 2022. "Conditional space-time pod extensions for stability and prediction analysis". *arXiv preprint arXiv:2207.04088*.

Touber, E. and Sandham, N.D., 2009. "Large-eddy simulation of low-frequency unsteadiness in a turbulent shock-induced separation bubble". *Theoretical and Computational Fluid Dynamics*, Vol. 23, pp. 79–107.

Vyas, M.A., Yoder, D.A. and Gaitonde, D.V., 2019. "Reynolds-stress budgets in an impinging shock-wave/boundary-layer interaction". *AIAA Journal*, Vol. 57, No. 11, pp. 4698–4714. doi:10.2514/1.J058487.

Wolf, W.R., 2011. *Airfoil Aeroacoustics: LES and Acoustic Analogy*. Ph.D. thesis, Stanford University.

Wolf, W.R., Azevedo, J.L.F. and Lele, S.K., 2012. "Convective effects and the role of quadrupole sources for aerofoil aeroacoustics". *Journal of Fluid Mechanics*, Vol. 708, p. 502–538. doi:10.1017/jfm.2012.327.

Wu, M. and Martín, M.P., 2008. "Analysis of shock motion in shockwave and turbulent boundary layer interaction using direct numerical simulation data". *Journal of Fluid Mechanics*, Vol. 594, p. 71–83. doi:10.1017/S0022112007009044.

8. Responsibility notice

The authors are solely responsible for the printed material included in this paper.